Self-Assembled Monolayers

DOI: 10.1002/anie.201205347

Parallel Imaging and Template-Free Patterning of Self-Assembled Monolayers with Soft Linear Microelectrode Arrays**

*Andreas Lesch, Britta Vaske, Frank Meiners, Dmitry Momotenko, Fernando Cortés-Salazar, Hubert H. Girault, and Gunther Wittstock**

Scanning electrochemical microscopy (SECM) has been used since its inception for imaging and surface modification in different modes.[1–6] The electrolytic generation of a reactive compound at the microelectrode (i.e. the SECM probe) allows the chemically well-defined transformation of various materials and layers that can be quantitatively controlled by adjusting the working distance, electrolysis current, and electrolysis time.[5,7] Particular versatile are modifications relying on the use of probe-generated Br_2 that may form HOBr upon disproportionation in alkaline or neutral solution. Br_2 and HOBr act as oxidants and have been used for semiconductor etching,[1,8] polyaniline deposition,[3] and the deactivation of enzyme layers.[2] Other probe-generated reagents include metal ions for metal deposition,[9,10] catalytically active metal ions,[11] and aryl diazonium salts.[6,12] The pH shift associated with nitrite oxidation was applied in the local etching of a thin Ni coating on a gold substrate in a chemical lens.[13] Kanoufi et al. reported the localized reduction of poly(tetrafluoroethylene)[14] and the oxidation of polystyrene[15] followed by further surface treatments. More recently, Hapiot et al. discovered that transient hydroxyl radicals $OH^{\bullet}$ can be used to remove organic coatings.[16] Particularly attractive is the possibility of performing surface modifications on samples immersed in aqueous buffer solution for the local manipulation of surface-bound biochemicals or adherent cells. This provides the opportunity to create local surface stimuli[17,18] or even dynamic stimuli, as popularized by the work of Mrksich and Yousaf,[19,20] but with the additional advantage that prepatterned surfaces are not required.[21–23]

However, the sequential nature makes all probe-induced modifications slow and presents a decisive disadvantage for many applications—even in the research laboratory. This problem has been addressed for scanning force microscopy (SFM) by the millipede[24] and parallel dip-pen nanolithography concepts.[25] Parallel electrode arrays have also been used with fixed arrangements of the individual electrodes but without lateral repositioning of the array.[26,27] The necessity of leveling samples relative to the horizontal (x,y) plane of the positioning system adds another technical difficulty that is especially evident for bent and rough samples.

Herein we demonstrate how the operation of individually addressable microelectrodes within a flexible electrode body can overcome many of these obstacles. These probes were introduced earlier for the imaging of metal-on-glass structures, human fingerprints, and enzyme activity.[28–30] The probe production starts with the formation of parallel microchannels with well-defined midpoint-to-midpoint distances (e.g. 250 μm or 500 μm) in a 100 μm thick polyethylene terephthalate (PET) film by laser ablation, filling the channels with a carbon ink, curing, and covering the entire probe with a 3 μm thick coating of Parylene C (see the Supporting Information for chemicals used (SI-1) and details of the probe fabrication (SI-2)). The cross-section of the carbon tracks defines the active electrode area and is exposed by mechanically cutting the layered structure. The individual electrodes have a distorted sickle shape (Figure 1 a). On account of the shrinking of the carbon ink, the tracks are recessed from the surrounding PET film. The array is mounted such that the Parylene C coating faces the sample with an inclination angle of 20° to the surface normal (Figure 1 b, SI-3). It "brushes" the sample during imaging and surface modification. However, since the electrode is recessed, mechanical or electrical contact between the carbon track and the samples is avoided.

The vertical position of the probe is set at 30–150 μm after the first mechanical contact between the probe and the sample (SI-4). Afterwards, the array probe is slid laterally across the surface as indicated by the arrow in Figure 1 b diminishing topographic artifacts in reactivity imaging.[31]

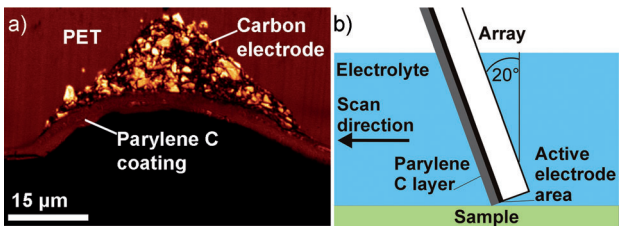

Figure 1. a) Cross-section of a carbon track forming the active area of an individual carbon electrode. b) The soft linear array slides above the sample during scanning in contact mode.

[*] A. Lesch, B. Vaske, F. Meiners, Prof. Dr. G. Wittstock
Institut für Reine und Angewandte Chemie
Carl von Ossietzky Universität Oldenburg
26111 Oldenburg (Germany)
E-mail: gunther.wittstock@uni-oldenburg.de
D. Momotenko, Dr. F. Cortés-Salazar, Prof. Dr. H. H. Girault
Laboratoire d'Electrochimie Physique et Analytique
Ecole Polytechnique Fédérale de Lausanne
Station 6, 1015 Lausanne (Switzerland)

[**] We thank Jan Ross and Jens Christoffers (Carl von Ossietzky Universität Oldenburg) for the preparation of the OEG-terminated thiol. This work is supported jointly by the Deutsche Forschungsgemeinschaft (Wi 1617/10) and the Fonds National Suisse pour la Recherche Scientifique (grant no. 20A21_121570/1) under the title "High- throughput SECM imaging". We thank Valérie Devaud and Cyrille Hibert (both EPFL) for technical assistance.

Supporting information for this article is available on the WWW under http://dx.doi.org/10.1002/anie.201205347.

When the array is moved in the opposite direction (repositioning during imaging), it is lifted off the sample until it is freely suspended in solution. For imaging areas larger than the width of the electrode array, several image frames can be tiled by the control software (SI-4).[29]

The pressure exerted by the probe on the sample is in the range of 10^3 N m^{-2}.[32] Although this value is not very precise because of difficulties in estimating the contact area between the probe and the substrate, it is around four orders of magnitude smaller than the pressure in standard SFM experiments.[33] Therefore, it should be possible to image delicate samples. This was verified by imaging a self-assembled monolayer (SAM) of hexadecanethiol formed by microcontact printing (μCP) square-shaped patterns on a gold substrate (Figure 2a). Imaging was performed in SECM feedback mode with a linear array of eight microelectrodes

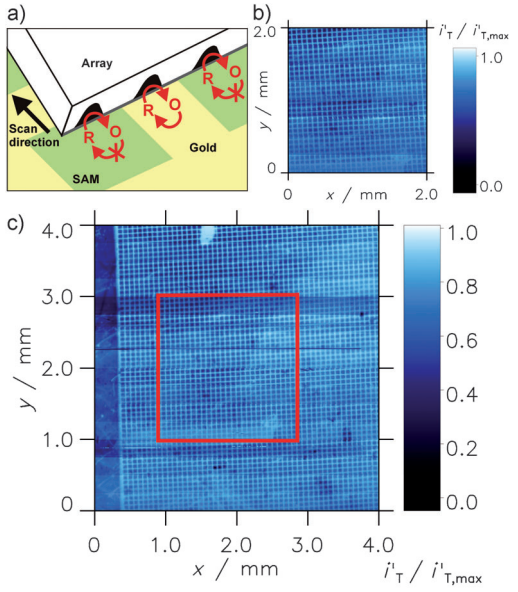

Figure 2. a) Schematic representation of SECM imaging over a μCP-SAM in feedback mode (not to scale). b) An area of 2 mm × 2 mm was scanned. c) Subsequently, a second image (4 mm × 4 mm) was recorded that included the frame of Figure 2b (red square).

(midpoint-to-midpoint distance 250 μm between of individual microelectrodes) in 2 mM ferrocenyl methanol. Figure 2b shows a 2 mm × 2 mm region of this pattern (imaging time 5.5 h) clearly resolving the stamped squares (50 μm × 50 μm) and showing imperfections in the pattern. Repeating this experiment with a larger image frame (4 mm × 4 mm, imaging time 7 h, Figure 2c) including the previously imaged region shows that no damage to the SAM occurred during the imaging. We expect the resolution to be slightly different in the *x* and *y* directions as a result of the asymmetric shape of individual probe electrodes. In the *y* direction the resolution is limited by the width of the individual microelectrodes (currently 30–50 μm). In the scanning direction (*x*), higher resolution is achieved thanks to the much smaller extension of the active electrode area of the probe along this axis (Figure 1a). Indeed, defects smaller than the stamped squares are clearly identified left of the stamped area in Figure 2c (see also SI-5.3). The SAM shows less permeability for the polar redox mediator, resulting in smaller currents than over the bare Au, where mediator recycling takes place. In order to compensate for unavoidable slight variations in electrode size, electrode shape, and working distance among the individual probe electrodes, the measured currents were calibrated to dimensionless currents (SI-5), in which 0.0 represents the minimum reduction current for that individual electrode (over the SAM region) and 1.0 stands for the maximum reduction current obtained with this electrode (over bare gold). Owing to the roughly constant working distance, the contrast of the entire image is almost uniform despite the fact that no attempt was made to align the sample surface to the (*x*,*y*) plane of the positioning system. A control experiment in which the SAM was gently scratched with a plastic Eppendorf pipette tip and then imaged showed that the probe is vulnerable to the mechanical removal of the SAM (SI-5).

Knowing that delicate SAMs are not mechanically damaged during imaging with the soft array probes, we electrogenerated Br_2/HOBr as an etchant from Br^--containing electrolytes in order to modify locally an oligo(ethylene glycol)-terminated SAM (OEG-SAM). $HS(CH_2)_{11}(OCH_2CH_2)_6OH$ used to synthesize the SAM was prepared according to Ref. [34]. While a potential pulse of $E_T = +1.8$ V was applied for 5 s, a current of 400–1000 nA generates Br_2/HOBr at the resting probe. Br_2/HOBr diffuses from the sickle-shaped microelectrodes towards the sample where it reacts with the OEG units and degrades them much faster than the alkyl chains of the SAM.[35] Because the etchant precursor Br^- and the redox mediator $[Ru(NH_3)_6]^{3+}$ are present in the electrolyte solution, the array could be used for a fast inspection experiment similar to Figure 2. OEG-SAMs are initially impermeable (passivated) for the mediator, which results in low currents over intact SAMs. This passivation is lifted after the reaction of the SAM with Br_2/HOBr, generating higher currents in SECM feedback images. Since the shape of the active electrode area is elongated, an image of the modified region might be distorted owing to a convolution of the sample and probe shapes. Therefore, a conventional Pt microdisk electrode was used and showed a D-shaped modified region (Figure 3a). The site-selective adsorption of a fluorescently labeled extracellular matrix protein on the modified regions of the SAM was detected by confocal laser scanning microscopy (CLSM, Figure 3b). The successful adsorption of an extracellular matrix protein should be applicable for site-controlled cell adhesion. The successful modification was also evident from SFM images recorded using the pulsed force mode (PFM-SFM) in which surface-modified tips generate a hydrophobicity/hydrophilicity contrast between pristine and modified OEG-SAMs (Figure 3c, SI-6). Since PFM-SFM provides much higher lateral resolution than SECM, the shape of the modified region can be clearly identified. It varies slightly depending on the particular electrode used for the modification. The minimum extension of the modified regions is roughly defined by the shape of the probe used (as shown Figure 1a). Additionally, diffusion of the electrogenerated Br_2/HOBr during the 5 s potential pulse contributes to the broadening of

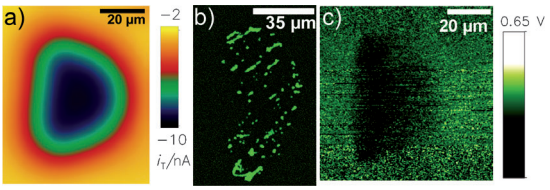

Figure 3. a) SECM feedback image using a conventional Pt microelectrode, $r_T = 12.5$ μm. b) CLSM image of selectively adsorbed fibrinogen–AlexaFluor488 on a modified area. c) PFM-SFM image of the adhesion forces reflecting the hydrophobicity of the modified spot. The images in (a)–(c) are from different measurements.

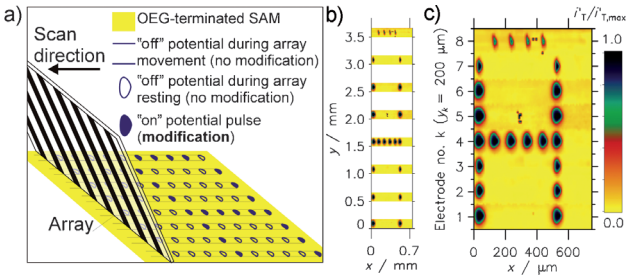

Figure 4. a) Schematic representation of surface modification during a line scan on OEG-SAM. For modification an "on" potential is applied with a defined pulse length. b) The capital letter "A" was patterned and scanned afterwards in SECM feedback mode using the same array and solution. c) Only the modified areas were scanned and plotted together excluding the nonscanned areas.

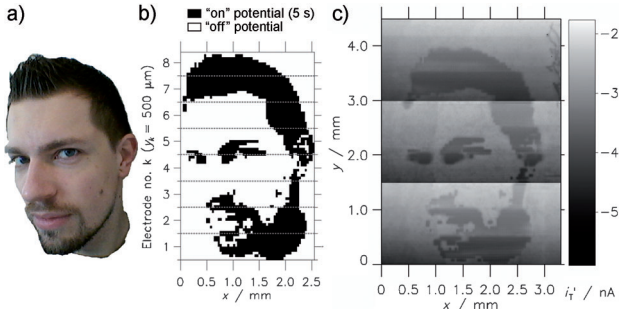

Figure 5. Drawing and reading of a pixel image in the OEG-terminated SAM. The optical photograph (a) was converted into black-and-white image with 69×80 pixels and an assumed spot size of 37.5 μm×50 μm (b). Modification of a closed area of 2.5 mm×4 mm was performed with eight microelectrodes. c) Readout of the image in SECM feedback mode by three microelectrodes of the array.

the modified regions, which can, however, be restricted by shorter pulses in combination with a higher concentration of KBr in the electrolyte. As a result of the geometry of the probe–sample arrangement, the effective working distance is smallest at the contact point between probe body and sample (left side in Figure 3c). The PET film of the probe forms an obstacle for the diffusion of the etchant and results in a sharper transition between the modified and unmodified regions. This difference is identified in the PFM-SFM images when the sharp left boarder in Figure 3c is compared to the curved and blurred right edge. Interestingly, the SAM permeability and protein adsorption in Figure 3a and b do not show the same trend. We had noted earlier that graduations in permeability were not necessarily reflected in the same trend for protein adsorption and cell adhesion.[36]

Higher throughput for surface modification was achieved by a dedicated routine of the in-house control software SECMx for which the step size and two potential values are defined in the software interface. One potential value is used for Br_2/HOBr generation ("on" potential). The other potential ("off" potential) is selected such that no reagent is formed at the probe and used during mechanical translation. After each mechanical step, the "on" potential is applied to each individual electrode for a duration (e.g. 5 s) specified in a pattern definition file (Figure 4a). A value of 0 s stands for maintaining the "off" potential at that position (no modification).

The character "A" was written in 58 s using this procedure. The distances between the spots perpendicular to the scanning direction are defined by the separation of the individual electrodes in the array (500 μm in this example). High-throughput SECM imaging was carried out with the same array providing the shape of each spot (Figure 4b) within 26 min when nonmodified areas were not scanned in order to accelerate the experiment. The imaged areas from Figure 4b were arranged into one image (Figure 4c), which gives a concise overview of the achieved quality of each individual "pixel".

The formation of larger and more complex patterns is demonstrated in Figure 5. A digital photograph (Figure 5a) was converted into a two-level image of 69×80 pixels (Figure 5b). The 80 pixels in the *y* direction correspond to 10 line scans performed with the eight individual electrodes of one array (500 μm electrode separation) within 87 min. Each line scan had 69 resting positions for surface modification. The step sizes were selected from the dimensions of the modified region in Figure 3c in such a way that with constant pulse duration neighboring regions overlap to form continuous modified areas instead of individual spots (SI-7). An SECM image of the modified region (readout) was recorded within 6.5 h by three electrodes of the same array using a smaller step size (SI-7) in order to achieve higher resolution (Figure 5c).

In conclusion, soft linear arrays of carbon microelectrodes were used in a simple method for the high-throughput, local electrochemical modification of surfaces. The array probes could also be applied to numerous electrochemical micropatterning procedures. The commercially available potentiostat used allows the control of up to 32 working electrodes with one auxiliary and one reference electrode and can be expanded to the parallel operation of 256 electrodes. Use of an array of this size would further speed up the procedures. The deposition of noble metals like Pt on the carbon electrodes would enable the electrogeneration of a greater variety of reagents. As demonstrated by SECM experiments with patterned SAMs, the weak forces exerted by the brushing probe indicate that it may be possible to image cultured cells and tissue samples. This could enable electrochemical analysis of tissues in the square-centimeter range for imaging drug distribution in cancer tissue[37,38] or for screening

for disorders in redox metabolism. Providing dynamic stimuli to cultured cell networks with soft probes could be a further interesting application. Microchannels for the release and aspiration of electrolyte solutions integrated into the soft probe body open up additional possibilities for modifying dry surfaces[39] and the delivery of different reagents to individual electrodes for the creation of different functionalities in one modification step; this is further supported by the option of different and more complex potential programs for each electrode and pixel. Owing to the multitude of further possibilities we expect that soft probes will lead to new approaches for electrochemical surface modification in addition to their proven applicability as analytical tools.

Received: July 6, 2012
Published online: September 17, 2012

Keywords: electrochemistry · scanning electrochemical microscopy · self-assembly · soft linear microelectrode arrays · surface modification

[1] D. Mandler, A. J. Bard, *J. Electrochem. Soc.* **1989**, *136*, 3143.
[2] H. Shiku, T. Takeda, H. Yamada, T. Matsue, I. Uchida, *Anal. Chem.* **1995**, *67*, 312.
[3] K. Borgwarth, C. Ricken, D. G. Ebling, J. Heinze, *Ber. Bunsen-Ges.* **1995**, *99*, 1421.
[4] T. Wilhelm, G. Wittstock, *Electrochim. Acta* **2001**, *47*, 275.
[5] S. Nunige, R. Cornut, H. Hazimeh, F. Hauquier, C. Lefrou, C. Combellas, F. Kanoufi, *Angew. Chem.* **2012**, *124*, 5298; *Angew. Chem. Int. Ed.* **2012**, *51*, 5208.
[6] C. Cougnon, F. Gohier, D. Belanger, J. Mauzeroll, *Angew. Chem.* **2009**, *121*, 4066; *Angew. Chem. Int. Ed.* **2009**, *48*, 4006.
[7] D. Mandler in *Scanning Electrochemical Microscopy* (Eds.: A. J. Bard, M. V. Mirkin), Marcel Dekker, New York, **2001**, p. 593.
[8] M. Sheffer, D. Mandler, *J. Electrochem. Soc.* **2008**, *155*, D203.
[9] S. Sauter, G. Wittstock, *J. Solid State Electrochem.* **2001**, *5*, 205.
[10] E. Malel, J. Colleran, D. Mandler, *Electrochim. Acta* **2011**, *56*, 6954.
[11] S.-Y. Ku, K.-T. Wong, A. J. Bard, *J. Am. Chem. Soc.* **2008**, *130*, 2392.
[12] M. Kongsfelt, J. Vinther, K. Malmos, M. Ceccato, K. Torbensen, C. S. Knudsen, K. V. Gothelf, S. U. Pedersen, K. Daasbjerg, *J. Am. Chem. Soc.* **2011**, *133*, 3788.
[13] J. Ufheil, F. M. Boldt, M. Börsch, K. Borgwarth, J. Heinze, *Bioelectrochemistry* **2000**, *52*, 103.
[14] C. Combellas, F. Kanoufi, D. Mazouzi, A. Thiebault, *J. Electroanal. Chem.* **2003**, *556*, 43.
[15] N. Ktari, C. Combellas, F. Kanoufi, *J. Phys. Chem. C* **2011**, *115*, 17891.
[16] J.-M. Noël, A. Latus, C. Lagrost, E. Volanschi, P. Hapiot, *J. Am. Chem. Soc.* **2012**, *134*, 2835.
[17] C. S. Chen, M. Mrksich, S. Huang, G. M. Whitesides, D. E. Ingber, *Science* **1997**, *276*, 1425.
[18] M. Mrksich, *Chem. Soc. Rev.* **2000**, *29*, 267.
[19] M. N. Yousaf, B. T. Houseman, P. M. Mrksich, *Angew. Chem.* **2001**, *113*, 1127; *Angew. Chem. Int. Ed.* **2001**, *40*, 1093.
[20] D. K. Hoover, E.-j. Lee, E. W. L. Chan, M. N. Yousaf, *ChemBioChem* **2007**, *8*, 1920.
[21] H. Kaji, K. Tsukidate, T. Matsue, M. Nishizawa, *J. Am. Chem. Soc.* **2004**, *126*, 15026.
[22] H. Kaji, M. Hashimoto, M. Nishizawa, *Anal. Chem.* **2006**, *78*, 5469.
[23] C. Zhao, I. Witte, G. Wittstock, *Angew. Chem.* **2006**, *118*, 5595; *Angew. Chem. Int. Ed.* **2006**, *45*, 5469.
[24] P. Vettiger, M. Despont, U. Drechsler, U. Durig, W. Haberle, M. I. Lutwyche, H. E. Rothuizen, R. Stutz, R. Widmer, G. K. Binnig, *IBM J. Res. Dev.* **2000**, *44*, 323.
[25] K. Salaita, Y. Wang, J. Fragala, R. A. Vega, C. Liu, C. A. Mirkin, *Angew. Chem.* **2006**, *118*, 7378; *Angew. Chem. Int. Ed.* **2006**, *45*, 7220.
[26] L. Zhang, X. Z. Ma, M. X. Lin, Y. Lin, G. H. Cao, J. Tang, Z. W. Tian, *J. Phys. Chem. B* **2006**, *110*, 18432.
[27] F. Deiss, C. Combellas, C. Fretigny, N. Sojic, F. Kanoufi, *Anal. Chem.* **2010**, *82*, 5169.
[28] F. Cortés-Salazar, D. Momotenko, H. H. Girault, A. Lesch, G. Wittstock, *Anal. Chem.* **2011**, *83*, 1493.
[29] F. Cortés-Salazar, D. Momotenko, A. Lesch, G. Wittstock, H. H. Girault, *Anal. Chem.* **2010**, *82*, 10037.
[30] D. Momotenko, L. Qiao, F. Cortés-Salazar, A. Lesch, G. Wittstock, H. H. Girault, *Anal. Chem.* **2012**, *84*, 6630.
[31] F. Cortés-Salazar, M. Träuble, F. Li, J.-M. Busnel, A.-L. Gassner, M. Hojeij, G. Wittstock, H. H. Girault, *Anal. Chem.* **2009**, *81*, 6889.
[32] A. Lesch, D. Momotenko, F. Cortes-Salazar, I. Wirth, U. M. Tefashe, F. Meiners, B. Vaske, H. H. Girault, G. Wittstock, *J. Electroanal. Chem.* **2012**, *666*, 52.
[33] E. Meyer, H. J. Hug, R. Bennewitz, *Scanning Probe Microscopy: The Lab on a Tip*, Springer, Berlin, **2004**.
[34] R. Jogireddy, I. Zawisza, G. Wittstock, J. Christoffers, *Synlett* **2008**, 1219.
[35] I. Brand, M. Nullmeier, T. Klüner, R. Jogireddy, J. Christoffers, G. Wittstock, *Langmuir* **2010**, *26*, 362.
[36] C. Zhao, I. Zawisza, M. Nullmeier, M. Burchardt, M. Träuble, I. Witte, G. Wittstock, *Langmuir* **2008**, *24*, 7605.
[37] M. L. Reyzer, Y. Hsieh, K. Ng, W. A. Korfmacher, R. M. Caprioli, *J. Mass Spectrom.* **2003**, *38*, 1081.
[38] U. Karst, *Angew. Chem.* **2004**, *116*, 2530; *Angew. Chem. Int. Ed.* **2004**, *43*, 2476.
[39] D. Momotenko, F. Cortes-Salazar, A. Lesch, G. Wittstock, H. H. Girault, *Anal. Chem.* **2011**, *83*, 5275.

